

Unsupervised Anomaly Detection in Time-series: An Extensive Evaluation and Analysis of State-of-the-art Methods

Nesryne Mejri, Laura Lopez-Fuentes, Kankana Roy, Pavel Chernakov, Enjie Ghorbel, and Djamila Aouada

Abstract—Unsupervised anomaly detection in time-series has been extensively investigated in the literature. Notwithstanding the relevance of this topic in numerous application fields, a complete and extensive evaluation of recent state-of-the-art techniques is still missing. Few efforts have been made to compare existing unsupervised time-series anomaly detection methods rigorously. However, only standard performance metrics, namely precision, recall, and F1-score are usually considered. Essential aspects for assessing their practical relevance are therefore neglected.

This paper proposes an original and in-depth evaluation study of recent unsupervised anomaly detection techniques in time-series. Instead of relying solely on standard performance metrics, additional yet informative metrics and protocols are taken into account. In particular, (1) more elaborate performance metrics specifically tailored for time-series are used; (2) the model size and the model stability are studied; (3) an analysis of the tested approaches with respect to the anomaly type is provided; and (4) a clear and unique protocol is followed for all experiments. Overall, this extensive analysis aims to assess the maturity of state-of-the-art time-series anomaly detection, give insights regarding their applicability under real-world setups and provide to the community a more complete evaluation protocol.

Index Terms—Time-series, Unsupervised Anomaly Detection, Evaluation Study.



1 INTRODUCTION

A Multivariate time-series corresponds to a temporally ordered set of variables. This mathematical representation has been used in countless domains such as finance, health, and biomechanics. Designing methods for automatically analyzing time-series (e.g. forecasting, classification, anomaly detection) has been widely investigated by researchers [6], [9]. A particular focus is given to anomaly detection in time-series [15]. In general, an anomaly or outlier can be defined as an observation or sample that does not follow an expected pattern. The popularity of anomaly detection in time-series is probably due to its interest in numerous industrial contexts. As an example, one can mention the detection of faulty sensors [23], fraudulent bank transactions [7], and pathologies in medical data [22].

In the literature, some attempts have been made to develop supervised and semi-supervised approaches [8], [10]. Nevertheless, the task of time-series anomaly detection is usually formulated as an unsupervised problem [20]. In fact, since anomalies occur rarely, annotating data becomes challenging and costly. In this article, we focus on the topic of unsupervised anomaly detection in time-series.

Earlier methods for anomaly detection in time-series have mostly employed traditional machine learning [17], [18] and auto-regressive [16], [19] techniques. However, as discussed in [3], these approaches are mainly subject to the *curse of dimensionality*. In other words, their performance

drops in the presence of high-dimensional time-series.

To address this, motivated by the tremendous advances in Deep Learning (DL), massive efforts have been recently made to design suitable Neural Network (DNN) architectures [2], [5], [26]. These DL-based approaches have achieved impressive performance in terms of *standard performance metrics* (precision, recall, and F1-score). Nevertheless, despite their promising results, their suitability in a realistic industrial context still needs further investigation. For that purpose, it is timely to propose an extensive comparison of recent DL techniques that considers the following aspects:

(1) Model size and model stability: Some important metrics for comparing DNNs in a real-world context are usually not reported. Existing methods overlook the *model size* and the *model stability*. By stable model, we mean a model which has stable performance under different training trials.

(2) Unified experimental protocol: There is no clear experimental protocol for evaluating state-of-the-art methods. As a consequence, it can be noted that the reported experimental values vary considerably from one paper to another. For instance, as highlighted in [1], a peculiar evaluation protocol called point adjustment [2] is often used [24], [26], while it is ignored in other cases [33], [34].

(3) Performance metrics for time-series: As discussed in [59], the used standard performance metrics (precision, recall, and F1-score) might not be entirely adequate for evaluating time-series anomaly detectors. These metrics were initially designed for time-independent predictions and not for range-based ones. As an alternative, Tatbul et al. [59] extended these metrics to time-series. However, it can be noted that current state-of-the-art methods do not consider these relatively novel evaluation criteria.

• All authors are affiliated to the Computer Vision, Imaging & Machine Intelligence Research Group (CVP) at the Interdisciplinary Centre for Security, Reliability and Trust (SnT), University of Luxembourg

E-mail: name.surname@uni.lu

Paper	Standard performance metrics	Performance metrics for time-series [59]	Network size	Evaluation of recent techniques	Analysis w.r.t anomaly type	Unified experimental protocol	Model stability
[3]	✓	✗	✗	✓	✗	✗	✗
[41]	✓	✗	✗	✗	✓	✓	✗
[1]	✓	✗	✗	✓	✗	✓	✗
This work	✓	✓	✓	✓	✓	✓	✓

TABLE 1: Comparison of existing evaluation studies of anomaly detection in time-series: we specify which of the following aspects were taken into account: (1) standard performance metrics which correspond to the precision, recall, and F1-score; (2) revisited performance metrics extending the precision, recall, and F1-score to time-series introduced in [59]; (3) network size; (4) evaluation of recent deep learning techniques; (5) analysis with respect to the types of anomalies; and (6) use of a unified experimental protocol.

(4) Experimental analysis with respect to the anomaly type: a detailed experimental evaluation with respect to the type of anomaly is missing in the state-of-the-art. Significant efforts have been dedicated to rigorously defining the different possible types of outliers in time-series [3], [41]. However, no concrete experimental analysis has been carried out in that direction.

In the literature, few evaluation studies for comparing recent anomaly detection algorithms [1], [3], [41] have been conducted. For instance, Choi et al. [3] present a brief comparison of recent DL algorithms in terms of precision, recall, and F1-score but neglect the model size and model stability. We can also mention the work of Lai et al. [41], where a new taxonomy for time-series outliers is proposed. Then, based on that, a methodology to generate synthetic datasets is suggested. They finally compare 9 different algorithms according to the outlier types but do not include the latest DL algorithms. Moreover, similar to [3], they only focus on classical evaluation criteria. Finally, Kim et al. [1] present a rigorous evaluation of recent DL techniques by questioning the point adjustment protocol. Nevertheless, the model size and model stability as well as the performance metrics for time-series are not considered.

Hence, in this survey, we provide a comprehensive evaluation study of state-of-the-art algorithms by taking into account all the mentioned aspects (1) to (4). As summarized in Table 1, standard performance metrics, as well as the novel performance metrics proposed in [59] are considered. In addition, the number of parameters of DL-based approaches is reported as it directly impacts the memory consumption and the model scalability. Moreover, experiments according to the nature of anomalies are carried out using the taxonomy that was recently introduced in [41]. Lastly, a unified experimental protocol is used to compare existing methods. This in-depth evaluation study will help the community understand the advantages and limitations of state-of-the-art techniques from a broader applicative perspective and lay the foundations for better experimental evaluation practices.

The remainder of this paper is organized as follows. Section 2 presents preliminaries necessary for the understating of this paper. Section 3 reviews state-of-the-art time-series anomaly detection methods. Section 4 describes the used datasets and details the evaluation protocol considered in the experiments. Section 5 presents and analyzes the results. Finally, Section 6 concludes this work.

2 PRELIMINARIES

A time-series is a temporally ordered set of n variables which can be denoted by $X = \{X_t\}_{1 \leq t \leq N}$ where $X_t \in \mathbb{R}^n$ refers to the n -dimensional vector of variables at an instant t . Note that the time-series is univariate if $n = 1$, and is multivariate otherwise ($n > 1$). This section reviews the necessary background for a better understanding of this survey. Specifically, we start by recalling the different types of time-series anomalies according to the taxonomy of [59]. Then, we present the usual paradigms employed for anomaly detection in time-series.

2.1 Types of anomalies

As discussed in [3], anomalies in time-series can generally be classified into three main categories, namely, *point*, *contextual*, and *collective* anomalies. However, unlike point anomalies, the definitions of contextual and collective ones are more ambiguous in the state-of-the-art, as stated in [41]. Indeed, they are heavily impacted by the application context. For instance, Yu et al. [29] define contextual anomalies as small temporal segments formed by neighboring points, while Golmohammadi et al. [30] consider them as seasonal points (occurring periodically). Lai et al. have recently refined the definition of outlier types [41]. They distinguish between *point-wise outliers* and *pattern-wise outliers*. The former is formed by *global* and *contextual outliers* while the latter is composed of *shapelet*, *seasonal*, and *trend outliers*. In the following, the taxonomy proposed in [41], which is central to our analysis, is recalled.

2.1.1 Point-wise anomalies

Point-wise outliers are local anomalies occurring on individual time stamps. Let $X = \{X_t\}_{1 \leq t \leq N}$ be a multivariate time-series and \hat{X}_t the expected value of X_t at an instant t according to a regression model. Given a well-chosen threshold $\delta > 0$, an anomaly at an instant t can be formally defined by,

$$\|X_t - \hat{X}_t\| > \delta, \quad (1)$$

where $\|\cdot\|$ defines an L_p norm.

Global outliers. They can be seen as point-wise anomalies which importantly deviate from the rest of the points in a time-series. They usually correspond to spikes in the time-series, as shown in Fig. 1a. In this case, the threshold δ can be formulated as,

$$\delta = \lambda \sigma(X), \quad (2)$$

where $\sigma(\cdot)$ refers to the standard deviation operator and $\lambda \in \mathbb{R}^{+*}$.

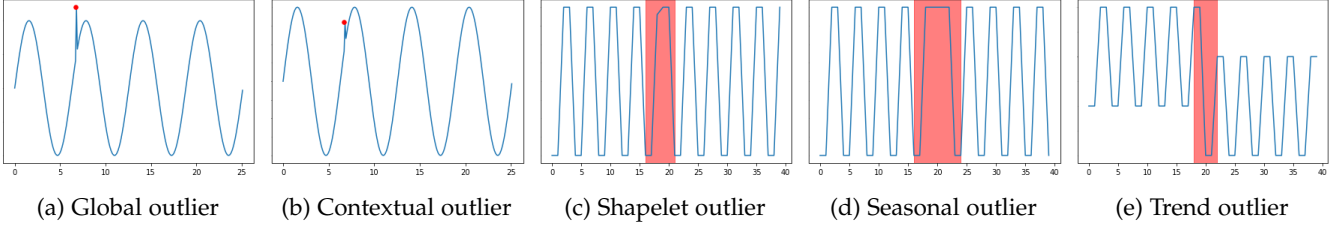


Fig. 1: Examples of the 5 different types of anomalies proposed in [41].

Contextual outliers. They refer to individual points which differ significantly from their neighbors. The latter are often small glitches in the time-series as illustrated in Fig. 1b. The threshold can be defined as,

$$\delta = \lambda \sigma(X_{t-k:t+k}), \quad (3)$$

where $X_{t-k:t+k} = \{X_{t-k}, X_{t-k+1}, \dots, X_{t+k}\}$ is the signal corresponding to the temporal window centered on t . The function $\sigma(\cdot)$ refers to the standard deviation operator and $\lambda \in \mathbb{R}^{+*}$.

2.1.2 Pattern-wise anomalies

Pattern-wise anomalies refer to anomalous sub-sequences which typically showcase discords or irregularities. These anomalies are defined in [41] by modeling a time-series X with spectral structural analysis [61] as follows,

$$X = \rho(2\pi\omega T) + \tau(T), \quad (4)$$

such that $\rho(2\pi\omega T) = \sum_k [A \sin(2\pi\omega_k T) + B \cos(2\pi\omega_k T)]$ corresponds to the base *shapelet* function which can be interpreted as the characteristic shape of X . The *seasonality*, which describes a pattern occurring at specific regular intervals in a time-series, is modeled with $w = \{w_1, w_2, \dots, w_k\}$. Finally, a trend function denoted by τ defines the global direction of X . In particular, a sub-sequence $X_{i:j}$ of a time-series X with $1 \leq i < j \leq N$ can be formulated using a shapelet function such that,

$$X_{i:j} = \rho(2\pi\omega T_{i,j}) + \tau(T_{i,j}), \quad (5)$$

with ρ , ω , τ , and $T_{i,j}$ respectively being the shape, the seasonality, the trend, and the time-stamps of the sub-sequence. The analysis of the shapelet, the seasonality as well as the trend functions allow distinguishing the three following outliers:

Shapelet outliers. They represent the anomalous sub-sequences enclosing shapelets that are different from the expected ones, as shown in Fig. 1c. The following condition can be used to define shapelet outliers as follows,

$$d_\rho(\rho(\cdot), \hat{\rho}(\cdot)) > \delta, \quad (6)$$

with d_ρ being a dissimilarity measure computed between two sets of shapelets. $\hat{\rho}(\cdot)$ corresponds to the expected shapelets in a given sub-sequence and δ is the threshold.

Seasonal outliers. They can be defined as sub-sequences with unexpected seasonalities with respect to the full sequence, as illustrated in Fig. 1d.

$$d_\omega(\omega, \hat{\omega}) > \delta, \quad (7)$$

with d_ω being a dissimilarity measure between two seasonality, $\hat{\omega}$ being the expected seasonality in the sub-sequence, and δ being the threshold.

Trend outliers. They refer to sub-sequences with an importantly altered trend. Consequently, a shift in the mean data can be observed, as shown in Fig. 1e. Mathematically, trend outliers can be defined by,

$$d_\tau(\tau, \hat{\tau}) > \delta \quad (8)$$

where d_τ is a dissimilarity measure computed between two trends, $\hat{\tau}$ is the expected trend of the sub-sequence, and δ is the threshold.

2.2 Paradigms for anomaly detection in times-series

Existing anomaly detection methods in time-series mainly employ five different paradigms, namely, clustering-based, density estimation-based, distance-based, reconstruction-based and forecasting-based methods.

2.2.1 Clustering-based methods

Let \mathcal{S}^n be the feature space of multivariate time-series of dimension n . Let \mathcal{N}^n be the estimated sub-space of normal time-series of dimension n such that $\mathcal{N}^n \subset \mathcal{S}^n$. Let f be a feature extractor function which maps an input time-series $X \in \mathbb{R}^{n \times N}$ to \mathcal{S}^n . An anomaly is detected if,

$$f(X) \notin \mathcal{N}^n. \quad (9)$$

Note that the classification of X as an anomaly or not can also be determined with the use of a distance that is compared to a threshold. This is the case, for example, of Support Vector Data Description (SVDD) [54], which measures the distance from the centroids.

2.2.2 Density estimation-based methods

Density estimation-based methods mainly aim to estimate the probability density function of normal time-series denoted as \mathbf{p}_θ . Given a time-series X , the likelihood function \mathcal{L} of θ and a threshold τ , an anomaly is detected if,

$$\mathcal{L}(\theta|X) > \tau. \quad (10)$$

2.2.3 Distance-based methods

Distance-based methods rely on the definition of an adequate distance between two temporal sequences. This distance should measure the dissimilarity between them. Let X and R be, respectively, a given time-series and a reference normal time-series. Let us denote by D a distance for time-series. Given a predefined threshold δ , an anomaly is detected in X if,

$$D(X, R) > \delta. \quad (11)$$

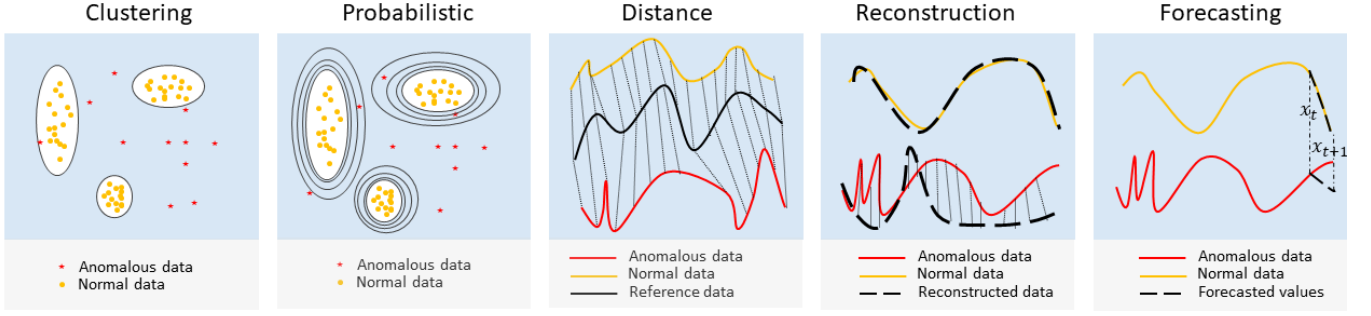


Fig. 2: Overview of the different paradigms for anomaly detection in time-series: in contrast to clustering and probabilistic approaches, distance-based, reconstruction-based and forecasting-based approaches take into account the temporal aspect.

2.2.4 Reconstruction-based methods

Reconstruction-based approaches aim at learning a model for the accurate and full reconstruction of a normal time-series. The assumption is that the learned model will fail when reconstructing abnormal sequences. Let X and \hat{X} be respectively the original and the reconstructed time-series. Given a predefined threshold δ , an anomaly is detected in X if,

$$\|X - \hat{X}\| > \delta. \quad (12)$$

2.2.5 Forecasting-based methods

Forecasting-based approaches are based on the prediction of future states given previous observations. Similar to reconstruction-based methods, they assume that the prediction will be less accurate in the presence of an anomaly. Let $X = \{X_0, X_1, \dots, X_N\}$ be a time-series where X_i refers to an observation of X at an instant i . Given a threshold δ , an anomaly is detected at an instant i if,

$$\|\hat{X}_i - X_i\| > \delta, \quad (13)$$

where \hat{X}_{t_i} corresponds to the predicted state given the observation $X_{0:i-1} = \{X_0, X_1, \dots, X_{i-1}\}$.

3 STATE-OF-THE-ART ON TIME-SERIES ANOMALY DETECTION

Over the last two decades, the research community has widely explored the field of anomaly detection in time-series. The latter can be addressed from five different perspectives. As reported in Section 2, we distinguish between clustering-based, density-estimation-based, distance-based, reconstruction-based, and forecasting-based techniques. Earlier techniques have investigated these five different paradigms by exploiting traditional machine learning [17], [18] and statistical tools [19]. Nevertheless, as mentioned in [3], these approaches have shown a drop in performance when dealing with high-dimensional time series. Given the recent advances in DL, DNNs have been considered as an alternative [24], [26], [33], [34], mainly taking inspiration from traditional methods. In the following, we review these five categories of approaches, starting with conventional techniques, then moving to current DL methods.

3.1 Clustering-based methods

Clustering-based methods are discriminative approaches aiming to estimate explicitly or implicitly decision boundaries for detecting anomalies [4], [49], [54] as depicted in Eq. 9. One-Class Support Vector Machine (OC-SVM) [4] is probably one of the most popular algorithms for anomaly detection. Its goal is to estimate the support of a high-dimensional distribution. This one-class classification method has been mainly used for detecting time-independent anomalies [56], [57] but has also been employed for isolating outliers in time-series [58]. Inspired by Support Vector Machines (SVM), Support Vector Data Description (SVDD) [54] is another well-known method that is often used in the context of anomaly detection [55]. Similar to SVM, kernels that map data representations to a higher dimensional space can be used. However, instead of relying on the estimation of a hyperplane, SVDD computes spherically shaped boundaries.

Shallow clustering-based approaches necessitate the hand-crafting of discriminative features and often require the selection of an appropriate kernel. Recently, with the advances in DL, there have been attempts to extend these classical approaches. Most of these methods, such as Deep SVDD [48] variants, extend traditional methods by learning a kernel that maps data to a discriminative high-dimensional feature space. This is usually carried out by optimizing a Neural Network. These approaches have shown promising results when dealing with non-sequential data. Unfortunately, the temporal modeling of time-series is often disregarded, mainly relying on a simple sliding window. As a solution, Shen et al. [25] suggest fusing multi-scale temporal features and employing a Recurrent Neural Networks (RNN) to model temporal dependencies.

3.2 Density-estimation methods

As described in Section 2.2.2, these probabilistic approaches detect anomalies by estimating the normal data density function. For example, Breunig et al. [50] proposed a method referred to as Local Outlier Factor (LOF) to detect anomalies by computing the local density. Tang et al. [53] calculate the local connectivity for determining anomalies instead. In [51] and [52], a Gaussian Mixture Model (GMM) and Kernel Density Estimation (KDE) are respectively used for estimating the density of normal representations. Over the last years, efforts have been made to introduce DNN-based probabilistic methods. For instance, Zong et al. [35]

proposed to train an auto-encoder for extracting relevant representations before fitting a GMM. Nevertheless, as for clustering-based methods, probabilistic approaches usually do not model the temporal aspect restricting their effectiveness in the context of time-series anomaly detection.

3.3 Distance-based methods

Distance-based methods usually define explicitly a distance between a time-series and a reference to detect anomalies [28], [37], [38], [39], as described in Section 2.2.3. Among the most used distance-based algorithm, one can refer to Dynamic Time Warping [40], which aims at finding the optimal match between two ordered sequences. Despite their relevance, distance-based methods have been less explored given their relatively high complexity induced by optimal matching and the need for defining a reference time-series [37].

3.4 Reconstruction-based methods

Reconstruction-based methods aim at reconstructing the entire time-series, as presented in Section 2.2.4. Shallow reconstruction-based time-series anomaly detection methods [42], [43], [44] have mainly adopted Principal Component Analysis [46] (PCA) or its variants such as kernel PCA (kPCA) [47]. These approaches estimate an orthogonal projection, then compute a reconstruction error between the original and reconstructed time-series. Lately, Auto-Encoders (AE) [45] have been introduced as the deep learning-based counterpart of PCA. Unsurprisingly, the latter has been adopted in the context of anomaly detection in time-series [32]. For example, Lin et al. [31] introduce a Long-Short Term Memory Variation Auto-Encoder (LSTM-VAE) architecture. While the Variation Auto-Encoder architecture (VAE) is used for learning robust representations, a Long Short-Term Memory (LSTM) network allows modeling temporal dependencies. Generative Adversarial Networks (GAN) have also been proposed as a reconstruction-based method. In [24], Audibert et al. attempted to take the best of both worlds. In particular, they introduced adversarially trained autoencoders for detecting anomalies in time-series.

3.5 Forecasting-based methods

As discussed in Section 2.2.5, traditional forecasting-based anomaly detection methods are primarily based on autoregression-based models such as AutoRegressive Integrated Moving Average (ARIMA) [36]. With the recent advances in deep learning, LSTM has been used to replace autoregression models [34]. This architecture allows modeling short-term as well as long-term temporal dependencies. Deng et al. [5] have recently proposed a graph-based deep learning model with an attention mechanism for capturing multivariate correlations.

3.6 Hybrid methods

As discussed in [14], reconstruction and forecasting-based approaches have shown to be, so far, the best candidates for anomaly detection in time-series. While reconstruction-based methods allow modeling inconsistencies within the

global distribution of time series, forecasting-based approaches are more appropriate for capturing local anomalies. For that reason, Zhao et al. [14] have introduced a hybrid method leveraging these two complementary paradigms. Specifically, they design a two-stream attention-based graph network that simultaneously optimizes forecasting and reconstruction losses.

4 DATASETS AND EVALUATION PROTOCOL

In this section, the datasets, the evaluation criteria, the pre-processing and post-processing algorithms as well as the considered methods for the experiments are presented.

4.1 Datasets

A total of five datasets have been considered for evaluating recent methods for anomaly detection in time-series. Table 2 details the different characteristics of each dataset. The considered benchmarks are:

Secure Water Treatment (SWaT). It is a dataset collected from a testbed water treatment for 11 days. During the last 4 days, 36 attacks of different duration and natures have been introduced. The data collected over the 7 first days have been used for training in all our experiments. During this period, the water treatment was carried out under normal conditions. In contrast, the data gathered during the last 4 days were exposed to multiple attacks. The latter have been used for testing¹.

Mars Science Laboratory (MSL). It is formed by 27 telemetry signals collected from the Curiosity Rover spacecraft on Mars. Each signal consists of a multivariate time-series of dimension 55. The first dimension encloses telemetry data, while the remaining 54 correspond to a one-hot encoded command. The publicly available dataset has been released by NASA [13]. The training and testing data are separated, and anomalies are annotated. Nevertheless, it can be noted that the experimental protocol varies from one reference to another. In particular, some studies such as [11] ignore the one-hot encoded vector considering only telemetry data. In addition, other approaches such as [5] combine the telemetric data from 27 signals assuming that it forms a unique dataset. Nevertheless, in most cases, authors do not provide sufficient information about their experimental protocol, making a direct comparison not straightforward. In this paper, we follow the experimental protocol of [12]. Each signal is considered to be a separate and independent multivariate sub-dataset. This means that the training and testing phases are performed each time on one single sub-dataset. Finally, the average performance is reported.

Soil Moisture Active Passive dataset (SMAP). This dataset contains telemetry data and one-hot encoded vectors similar to the MSL dataset. It has also been released by NASA [13]. However, in this case, the dataset is formed by 53 signals received from the Soil Moisture Active Passive satellite. The annotated training and testing data are provided. Nevertheless, as for the MSL dataset, similar inconsistencies regarding the experimental protocol can be remarked. For that reason, we propose using the protocol of [12], where each signal is considered to be a separate and independent

1. Details of the SWaT dataset can be found here

multivariate sub-dataset. This leads to train and test on 53 different sub-datasets and reporting the obtained average performance.

UCR time series anomaly archive (UCR). It has been recently proposed by Renjie and Keogh [21]. In [21], the authors claim that most of the existing anomaly detection datasets are *trivial*. By trivial, they mean that an anomaly can be detected with a single line of MATLAB code. They also criticize the lack of realism and annotation precision in current datasets. As an alternative, they introduce the UCR dataset, which gathers 250 realistic sub-datasets. This dataset is collected from various fields, including medicine, sports, and robotics. The training and test sets are well-defined².

Automated Time-series Outlier Detection System (TODS). It is a collection of 5 synthetically generated multivariate datasets. The dataset was generated using the source code from [41], therefore producing different types of anomalies following the taxonomy of [41]. The dimension of the generated time-series is 10. Training datasets contain only normal values, while testing datasets incorporate 5 different types of anomalies. The annotation of the outlier types is provided, therefore allowing a per-type analysis.

4.2 Evaluation criteria

In this section, we present the used evaluation criteria. **Precision, recall and F1-scores.** The most common metrics used to evaluate the performance of time-series anomaly detection algorithms are the precision computed as follows,

$$\text{Precision} = \frac{\text{True positives}}{\text{True positives} + \text{False positives}}, \quad (14)$$

the recall is calculated as below,

$$\text{Recall} = \frac{\text{True positives}}{\text{True Positives} + \text{False Negatives}} \quad (15)$$

and the F1-score corresponding to,

$$\text{F1-score} = \frac{2 \cdot \text{Precision} \cdot \text{Recall}}{\text{Precision} + \text{Recall}}. \quad (16)$$

Revisited precision, recall and F1-scores for time-series. In addition to conventional performance metrics, more recent and elaborate performance metrics tailored to time-series introduced in [59] are considered. These metrics extend classical precision, recall, and F1-score, from point-based to range-based anomaly detection. Fig. 3 highlights the distinction between point-based and range-based anomalies. Contrary to the case of point-based approaches, a prediction in a time-series can be both a true positive (TP) and a false negative (FN) due to *partial overlap* with the ground-truth as shown in Fig. 3 b. Therefore, as discussed in [59], a more informative time-series evaluation process should (1) quantify the size of the partial overlap; (2) identify the overlap position, and; (3) take into account its cardinality, i.e., with how many anomalous ground-truth sub-sequences it overlaps. More specifically, given a set of real anomaly sequences $R = \{R_1, \dots, R_{N_r}\}$ and a set of predicted anomaly sequences $P = \{P_1, \dots, P_{N_p}\}$ the recall is expressed with

respect to the number of real anomalies N_r in a dataset [59]. It seeks to reward a detector when it predicts a TP and penalizes it when the prediction is an FN as follows,

$$\text{Recall}_T(R, P) = \frac{1}{N_r} \sum_{i=1}^{N_r} \text{Recall}_T(R_i, P), \quad (17)$$

and,

$$\begin{aligned} \text{Recall}_T(R_i, P) = & \alpha \cdot \mathbb{1}_{\sum_{j=1}^{N_p} |R_i \cap P_j| \geq 1} \\ & + \frac{1 - \alpha}{\sum_{j=1}^{N_p} |R_i \cap P_j|} \cdot \mathcal{S}_c(R_i, P), \end{aligned} \quad (18)$$

where $0 \leq \alpha \leq 1$ is a scaling factor that rewards the detector when it detects the existence of the anomaly R_i and $\mathbb{1}$ is an indicator function. Finally, $\mathcal{S}_c(R_i, P)$ which quantifies the overlap size is computed based on the cumulative overlap size ω as follows,

$$\mathcal{S}_c(R_i, P) = \sum_{j=1}^{N_p} \omega(R_i, R_i \cap P_j, \delta), \quad (19)$$

where δ returns a score depending on the overlap location between R_i and a prediction P_j (flat bias, front bias, middle bias, and back bias). Further details could be found in the original manuscript [59]. The precision is similarly defined. It seeks to assess the quality of the predictions by rewarding a detector in the presence of a TP and penalizing it when facing an FP. It is computed as follows,

$$\text{Precision}_T = \frac{1}{N_p} \sum_{i=1}^{N_p} \text{Precision}_T(R, P_i), \quad (20)$$

and,

$$\text{Precision}_T(R, P_i) = \frac{1}{\sum_{j=1}^{N_r} |R_j \cap P_i|} \cdot \mathcal{S}(R, P_i), \quad (21)$$

where $\mathcal{S}_c(R, P_i)$ quantifies the cumulative overlap between the considered prediction P_i and all the ground-truths in R as explained in Equation (19). It is expressed as,

$$\mathcal{S}_c(R, P_i) = \sum_{j=1}^{N_r} \omega(P_i, P_i \cap R_j, \delta). \quad (22)$$

Finally, the F1-score is redefined as follows,

$$\text{F1-score}_T = \frac{2 \cdot \text{Precision}_T \cdot \text{Recall}_T}{\text{Precision}_T + \text{Recall}_T} \quad (23)$$

Model stability. We define model stability as the ability of a machine/deep learning algorithm to reproduce similar results when retrained under the same conditions. While OC-SVM ensures stability because of its deterministic nature, most of the considered methods rely on a random parameter initialization which may impact the final performance of the model. Ideally, the model should achieve the same results regardless of this initialization. To assess the stability, each experiment is carried out five times. Then, the mean and standard deviation of those five runs are reported. A lower standard deviation reflects higher stability. To the best of our knowledge, we are among the first to analyze this aspect experimentally in the context of anomaly detection in time-series.

2. More information about the UCR dataset can be found here

	SWaT	MSL	SMAP	UCR	TODS
Number of datasets	1	27	55	250	5
Variables	52	55	25	1	10
Percentage of anomalies	12.14	10.48	12.82	0.38	5
Training data points	495000	58317	138004	5302449	10000
Testing data points	449919	73729	435826	12919799	10000
Type of data	Real	Real	Real	Real	Synthetic
Type of anomalies	Artificially forced	Natural	Natural	Natural/Synthetic	Synthetic

TABLE 2: Summary of the 5 datasets used in the experiments. The percentage of anomalies in the testing set is reported.

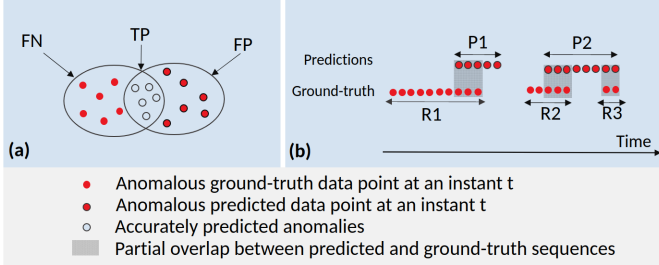


Fig. 3: The evaluation process of (a) point-based anomalies versus (b) range-based anomalies. Range-based anomalies are characterized by partial overlap(s) with the ground-truth. A more accurate evaluation for time-series should quantify the overlap in terms of **size**, **position**, and **cardinality**.

Generalization to different types of anomalies. We propose reporting the performance according to the anomaly type encountered. This analysis can help identify the most suitable algorithm for a given application. To that aim, the TODS benchmark, which encloses the annotation of 5 different types of outliers depicted in Section 4.1 is used. Although the definition of different anomaly types has been reported in several references, very few works have carried out an experimental study with respect to the anomaly type. A rare example we can mention is the work of [41]. Nevertheless, it can be noted that in this paper, recent DL-based state-of-the-art approaches such as GDN [5], USAD [24], and MTAD-GAT [14] are not evaluated. For each anomaly type, the percentage of well-detected anomalies is reported.

Model size. In a real-world context, deploying algorithms on specific hardware with a limited memory capacity can be challenging. Therefore, being aware of the model size, which directly impacts the memory consumption, is a crucial component often neglected. For that purpose, we report the number of parameters and the size in MegaBytes (MB) of the trained deep learning models considered for this evaluation.

4.3 Post-processing and Pre-processing

Data Normalization. Normalizing the data is a common practice in machine learning, particularly in anomaly detection. Hence, for the sake of fairness, a data normalization pre-processing was applied in all our experiments. More specifically, the data are normalized using the maximum and minimum values in the training data as in [14].

Point Adjustment. Point adjustment initially introduced in [2] is a protocol that adjusts the predictions before computing performance metrics. It acts as follows: if at least one point is classified as an anomaly in an outlier segment, all the predictions in that segment are set to anomalous. The idea behind this protocol is that an algorithm triggering an

GT	0 0 0 1 1 1 1 1 0 0 1 0 0 0 1 1 1 1 1 1 0 0 1 1 1
Pred	1 0 0 0 0 1 0 0 0 0 0 0 0 0 0 0 1 1 0 0 0 0 0 0 0
PA	1 0 0 1 1 1 1 1 0 0 0 0 0 0 1 1 1 1 1 1 0 0 0 0 0

Fig. 4: Application of the Point Adjustment (PA) on a given time-series: the Ground-Truth (GT), the original prediction (Pred) and the prediction after Point Adjustment (PA) are reported. In this example, the performance of the algorithm without and with point adjustment is respectively: Precision = 0.75, Recall = 0.2, F1-Score = 0.32, and Precision = 0.92, Recall = 0.79, F1-Score = 0.85. Best viewed in colors.

Method	Type of paradigm	Nature
OC-SVM [4]	Clustering	Shallow
iForest [49]	Clustering	Shallow
ARIMA [36]	Forecasting	Shallow
DA-GMM [35]	Density-estimation	Deep
THOC [25]	Clustering	Deep
USAD [24]	Reconstruction	Deep
GDN [5]	Forecasting	Deep
MTAD-GAT [14]	Hybrid (Forecasting & Reconstruction)	Deep

TABLE 3: Paradigm type and nature of evaluated methods

alert for any point in a contiguous anomaly segment might be sufficient for a timely reaction. Fig. 4 illustrates the point adjustment protocol by showing the ground-truth, the original predictions, and the predictions after point adjustment of a given time-series. After applying the point adjustment protocol, the F1-Score goes from 0.32 to 0.85. This significant gap has therefore raised some concerns in the literature regarding the use of point adjustment. For example, Kim et al. [1] claim that by using this protocol, a randomly generated anomaly score might outperform several recently proposed time-series anomaly detection algorithms. In this paper, we report the performance of existing methods with and without point adjustment.

4.4 Evaluated methods

We consider in total 8 anomaly detection methods. Table 3 summarizes the characteristics of each evaluated method.

Three shallow standard methods are evaluated, namely, OC-SVM [4], iForest [49] and ARIMA [36]. In addition, five recent DL-based methods have been considered: DA-GMM [35], THOC [25], USAD [24], GDN [5] and MTAD-GAT [14]. The latter has been selected according to the following criteria: (1) Relevance of the topic: all the chosen anomaly detection algorithms are unsupervised and have been specifically designed for detecting anomalies in time-series. (2) Publication date: all the DL-based algorithms are recent. In particular, they have been introduced between

Point adjustment		SWaT		MSL		SMAP		UCR		TODS		Avg. per method	
		Without	With	Without	With	Without	With	Without	With	Without	With	Without	With
USAD [24]	Precision	0.28±0.015	0.32±0.019	0.15±0.010	0.22±0.009	0.18±0.008	0.26±0.013	0.01±0.000	0.02±0.000	0.05±0.002	0.07±0.001	0.19±0.131	0.26±0.155
	Recall	0.74±0.014	0.89±0.029	0.57±0.051	0.99±0.015	0.49±0.008	0.95±0.014	0.48±0.002	0.95±0.003	0.54±0.017	0.71±0.016		
	F1-Score	0.41±0.019	0.47±0.024	0.21±0.015	0.33±0.013	0.21±0.006	0.34±0.015	0.02±0.000	0.04±0.000	0.10±0.003	0.13±0.003		
GDN [5]	Precision	0.34±0.034	0.40±0.047	0.31±0.012	0.39±0.016	0.25±0.002	0.36±0.011	0.12±0.003	0.31±0.009	0.07±0.007	0.10±0.018	0.27±0.141	0.42±0.140
	Recall	0.72±0.037	0.72±0.037	0.64±0.017	1.00±0.002	0.55±0.042	1.00±0.001	0.42±0.001	0.99±0.002	0.59±0.160	0.75±0.124		
	F1-Score	0.46±0.030	0.57±0.048	0.35±0.006	0.50±0.015	0.33±0.013	0.46±0.013	0.12±0.003	0.39±0.011	0.11±0.003	0.16±0.018		
THOC [25]	Precision	0.62±0.160	0.77±0.083	0.22±0.009	0.31±0.013	0.16±0.007	0.26±0.007	0.01±0.005	0.06±0.017	0.05±0.008	0.09±0.014	0.19±0.181	0.35±0.262
	Recall	0.46±0.130	0.86±0.020	0.46±0.017	0.87±0.015	0.27±0.009	0.84±0.017	0.00±0.009	0.06±0.020	0.19±0.033	0.35±0.059		
	F1-Score	0.52±0.140	<u>0.81±0.054</u>	0.25±0.009	0.41±0.015	0.12±0.008	0.34±0.008	0.00±0.001	0.06±0.019	0.08±0.14	0.14±0.023		
MTAD-GAT [14]	Precision	0.85±0.037	0.86±0.036	0.57±0.037	0.60±0.040	0.58±0.034	0.59±0.034	0.10±0.004	0.17±0.003	0.16±0.078	0.16±0.078	0.45±0.324	0.50±0.317
	Recall	0.90±0.033	0.96±0.032	0.79±0.030	0.86±0.034	0.87±0.029	0.91±0.030	0.28±0.008	0.57±0.017	0.01±0.017	0.01±0.017		
	F1-Score	0.87±0.014	0.90±0.014	0.60±0.032	0.64±0.035	0.65±0.033	0.67±0.034	0.13±0.005	0.25±0.005	0.02±0.027	0.02±0.027		
DAGMM [35]	Precision	0.43±0.000	0.49±0.000	0.12±0.006*	0.20±0.002*	0.11±0.008*	0.16±0.003	0.01±0.000	0.03±0.000	0.12±0.000	0.15±0.000	0.19±0.183	0.28±0.194
	Recall	0.71±0.000	0.90±0.002	0.19±0.004*	0.44±0.000*	0.17±0.010	0.41±0.000*	0.20±0.002	0.78±0.002	0.49±0.000	0.63±0.000		
	F1-Score	0.54±0.000	0.64±0.001	0.12±0.004*	0.25±0.002*	0.10±0.006*	0.19±0.002*	0.01±0.000	0.06±0.000	0.19±0.000	0.24±0.000		
OCSVM [4]	Precision	0.24±0.000	0.26±0.000	0.15±0.000	0.25±0.000	0.12±0.000	0.15±0.000	0.01±0.000	0.02±0.000	0.05±0.000	0.05±0.000	0.18±0.121	0.24±0.153
	Recall	0.85±0.000	0.95±0.000	0.66±0.000	0.95±0.000	0.66±0.000	0.85±0.000	0.73±0.000	0.85±0.000	0.85±0.000	0.85±0.000		
	F1-Score	0.37±0.000	0.41±0.000	0.24±0.000	0.40±0.000	0.20±0.000	0.26±0.000	0.02±0.000	0.04±0.000	0.09±0.000	0.09±0.000		
iForest [49]	Precision	0.23±0.097	0.26±0.118	0.18±0.041	0.47±0.037	0.10±0.008	0.34±0.009	0.05±0.006	0.16±0.006	0.05±0.012	0.17±0.057	0.14±0.116	0.34±0.131
	Recall	0.83±0.096	0.97±0.003	0.16±0.053	0.66±0.058	0.04±0.005	0.40±0.009	0.12±0.013	0.45±0.008	0.04±0.009	0.17±0.018		
	F1-Score	0.36±0.099	0.40±0.134	0.17±0.034	0.55±0.039	0.08±0.004	0.36±0.009	0.07±0.003	0.24±0.005	0.04±0.007	<u>0.17±0.023</u>		
ARIMA [36]	Precision	0.13±0.000	0.13±0.000	0.28±0.000	0.31±0.000	0.17±0.000	0.18±0.000	0.01±0.000	0.01±0.000	0.05±0.000	0.06±0.000	0.16±0.950	0.20±0.126
	Recall	0.99±0.000	1.00±0.000	0.83±0.000	1.00±0.000	0.82±0.000	0.96±0.000	0.85±0.000	0.97±0.000	0.69±0.000	0.87±0.000		
	F1-Score	0.23±0.000	0.23±0.000	0.28±0.000	0.39±0.000	0.19±0.000	0.24±0.000	0.02±0.000	0.02±0.000	0.09±0.000	0.11±0.000		
Avg. F1-score per dataset		0.47±0.177	0.55±0.209	0.28±0.138	0.43±0.117	0.23±0.173	0.36±0.141	0.05±0.048	0.14±0.128	0.09±0.047	0.13±0.060		

TABLE 4: Results in terms of traditional performance metrics of evaluated state-of-the-art methods (precision, recall, F1-score) on the 5 considered datasets. The experiments have been performed 5 times for each algorithm and dataset. The provided values correspond to the mean and standard deviation. The bold and underlined results correspond to the first and second-best F1-Score obtained for a particular dataset.

*DAGMM did not converge on sub-datasets from MSL and SMAP. Hence, the reported results for this particular method are only considering the sub-datasets on which DAGMM converged.

2018 and early 2022. (3) Impact: the chosen algorithms have been published in top-tier conferences and are highly cited papers from the field. (4) Code availability: the official codes of the selected algorithms are publicly available. (5) Diversity: methods from different paradigms have been considered. The only paradigm that was ignored is the distance-based since we were not able to find a deep learning approach falling in this category.

5 RESULTS

5.1 Performance using standard metrics

Best performing approach. Table 4 reports the performance of the evaluated methods using standard metrics (precision, recall, and F1-score) on the five considered datasets. For a more intuitive visualization of the results, Fig. 5 shows the F1-score. In general, MTAD-GAT [14] is the best-performing approach, surpassing other methods on four datasets, namely, SWaT, MSL, SMAP, and UCR. This can be explained by the fact that this approach is hybrid as it is based on forecasting and reconstruction losses. Indeed, this allows the simultaneous detection of local and global anomalies. Nevertheless, it can be remarked that the results obtained on TODS contradict this statement. Indeed, MTAD-GAT registers inferior performance on this benchmark as compared to other methods, including DL and conventional methods. Two hypotheses might justify this drop: (1) the TODS dataset encloses complex anomalies that are *moderately local* and are hardly captured by a simple forecasting and/or reconstruction approach, favoring probabilistic modeling as in DAGMM [35]. However, the higher performance obtained for GDN [5] and USAD [24] partly disprove this assumption; and (2) the synthetic data in TODS are not realistic, making them hardly predictable. Another observation that can be made is that GDN [5] presents the second-best performance on three datasets, namely MSL, SMAP, and UCR. This confirms the relevance of using graph representations for modeling time-series.

Surprisingly, graph-based approaches (GDN and MTAD-GAT) remain relatively effective on a univariate dataset (UCR), although modeling the connectivity between variables is unnecessary.

DL vs conventional methods. As reported in Table 4 and Fig. 5, DL methods, specifically MTAD-GAT and GDN, generally outperform conventional methods. For example, the superiority of DL approaches is extremely noticeable when comparing GDN and ARIMA, which are both forecasting techniques. This increase in performance can be explained by the fact that ARIMA struggles to model the dependencies between variables. However, the gap in performance between DL and traditional methods is less visible in some cases, contradicting the assumption of [3], which states that DL methods are more effective in the presence of high-dimensional time-series. For instance, OC-SVM shows comparable performance with several DL-based anomaly methods such as THOC and USAD on high-dimensional datasets. More precisely, OC-SVM achieves an F1-score of 0.24 and 0.2 on MSL and MSAP against 0.21 and 0.21 for USAD and 0.25 and 0.2 for THOC, respectively. Another observation that can be made is that conventional approaches, except iForest, seem to be suitable for applications where recall is more important than precision. An example of such an application could be the detection of debris among other objects in space [60]. On the contrary, DL approaches are overall more precise.

Impact of point adjustment. From the results of Table 4, it can be noted that the Point Adjustment (PA) process significantly boosts the performance. In particular, the highest performance gain can be observed for iForest on the MSL dataset, where the F1-score increases from 17% to 55%. This can be explained by the fact that PA adjusts the predictions before computing the metrics. The adjustment is made in a way that rewards a detector when detecting at least one instance of an anomalous segment. The intuition behind that is that finding one anomaly in a segment is sufficient for a timely reaction. Such an intuition closely impacts

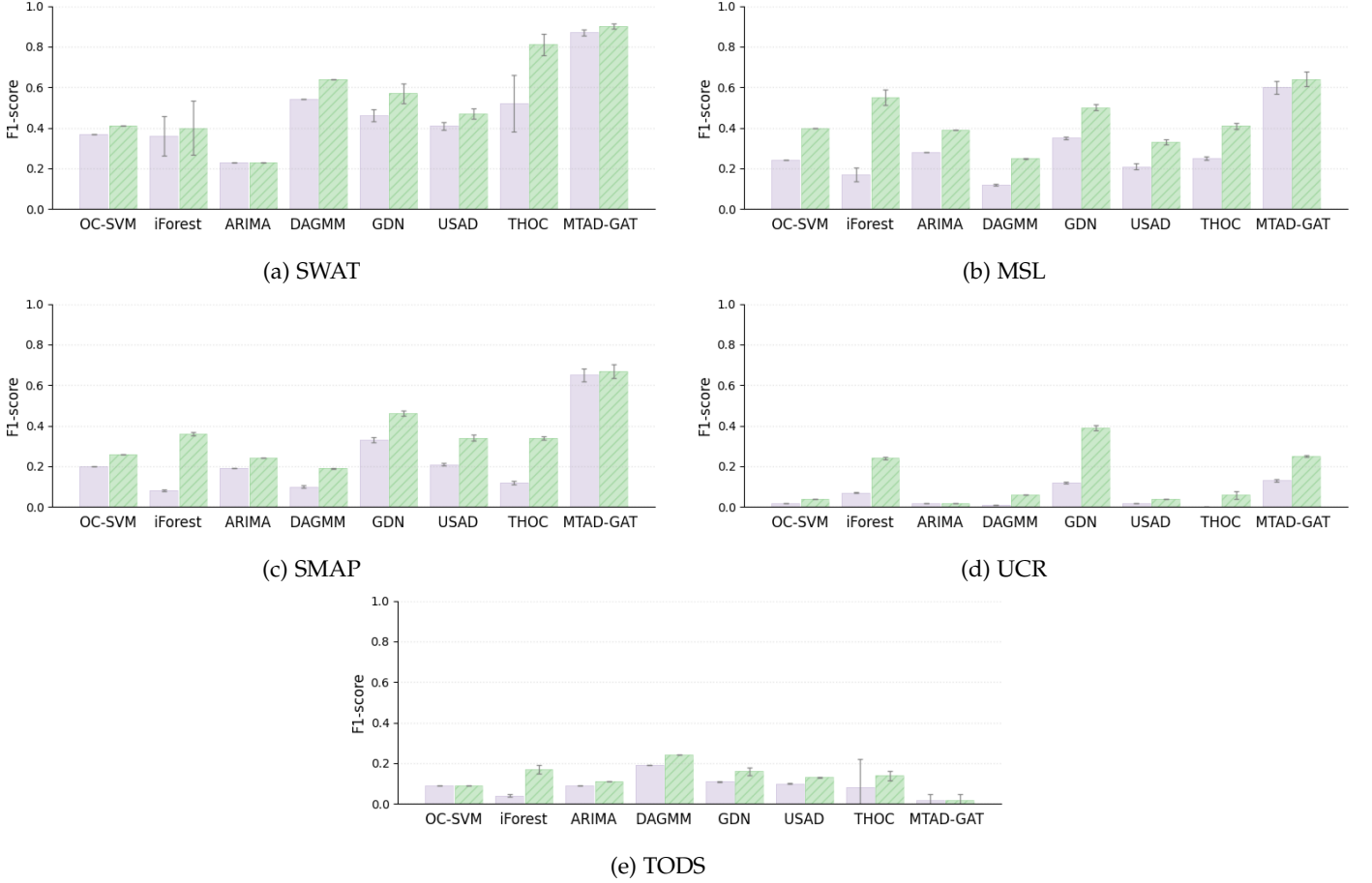


Fig. 5: Mean F1-Score on the five datasets. The non-hatched and hatched bars correspond to the mean F1-Score with and without Point Adjustment (PA), respectively. The vertical black line represents the standard deviation over five runs.

the recall since it increases the number of False Positives (FP). In addition, before applying PA, all DL approaches seem to be in general, more effective than conventional approaches. However, after PA, this is no longer the case. For example, iForest achieves comparable performance with THOC. Overall, PA seems to bias the analysis as it treats range-based data as punctual, neglecting the overlap size and the location of anomalies. Consequently, this blurs the applicability of detectors in real-life setups.

Benchmark complexity. All tested methods fail to detect effectively anomalies in UCR, although it is a univariate dataset. This might be due to its low ratio of anomalies. As discussed in Section 4.1, UCR is among the first benchmark to mimic a more realistic configuration, highlighting the difficulty of detecting rare anomalies. The rate of anomalies might have a significant role in defining the complexity of a given dataset. For natural anomalies, two observations could be made. First, the average performance on MSL and SMAP is comparable despite having a significantly different number of variables. Second, natural but induced/forced anomalies seem easy to detect, given that all methods perform well on the SWaT dataset. Unfortunately, such a scenario is unrealistic in most real-world scenarios as the anomalies are generally infrequent.

5.2 Performance using revisited metrics for time-series

Conventional metrics vs revisited metrics. Table 6 shows the results of evaluation using the revisited F1-score for time-series calculated using Recall_T and Precision_T proposed in [59].

It can be remarked that there exists a significant gap in performance between the results based on conventional and revisited metrics. One main reason is that the revisited metrics consider the overlap size between the predicted sequences and the ground-truth. In contrast, the traditional metrics do not take into account the sequential aspect nor quantify the overlap between the predictions and the ground-truth. Moreover, it can be noted that the results of the revisited metrics are not in full accordance with the conventional ones. On the one hand, GDN and USAD achieve more competitive results as compared to other approaches. On the other hand, the assumption about the superiority of the hybrid method no longer holds. Overall, both classical and DL forecasting-based techniques give the highest performance. This perspective suggests that the majority of anomalies in benchmarked datasets are local. Finally, DAGMM seems to be among the least effective methods, suggesting its inability to model the distribution of anomalies. This can be explained by the fact that anomalies do not necessarily follow a multimodal Gaussian distribution. Some observations can be made regarding the difficulty of each dataset. First, MSL seems slightly less

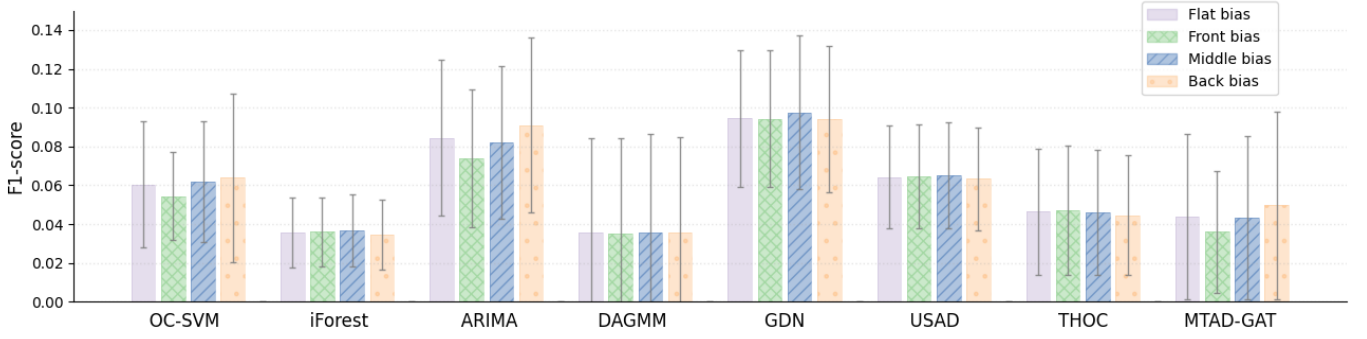


Fig. 6: The mean performance per method on all datasets using the range-based metrics [59], with different location biases.

challenging than SWAT. Second, in line with the results based on conventional metrics, the obtained performance suggests that natural anomalies are more straightforward to detect than synthetic ones. Two reasons could potentially explain that: (1) the datasets with natural anomalies have a high percentage of anomalies, and (2) synthetic datasets do not reliably reflect reality and do not include a sufficient number of anomalies.

Location bias. Herein, we analyze the results with and without location bias. Table 6, Table 7, Table 8, and Table 9 show the results using flat, front, middle and back bias, respectively. Fig. 6 depicts the overall performance for each method under different bias settings. Although the idea of location bias seems theoretically interesting and flexible for different domain-specific applications, it does not practically bring more information, as the results do not change importantly. However, it can be noted that the middle and back bias allowed the detection of more anomalies compared to flat and front. This suggests that most detectors remain immature for applications necessitating an early anomaly such as real-time intrusion detection [62] or cyberattack attempts via network activity [63].

DL vs conventional methods. Although the top-three best-performing methods are DL models (according to the conventional metrics), it can be seen that classical approaches such as OC-SVM can achieve comparable performance with its counterpart clustering DL approach, namely THOC. This suggests that conventional methods are not necessarily obsolete and that, depending on the application, they can be considered for anomaly detection.

Univariate vs multivariate. The results of Table 4 and Table 6 seem to be in accordance. Indeed, all methods seem to have poor performance on UCR, which is univariate, while on other multivariate datasets such as MSL, the performance is relatively higher.

5.3 Model stability

Besides reporting the precision, recall, and F1-score, it is interesting to observe the behavior of detectors when trained with different initializations. Table 4 and Fig. 5 report the performance average and standard deviation for every approach after five runs. Undoubtedly the most stable methods are the deterministic ones which are ARIMA and OC-SVM. Among DL approaches, DAGMM seems to be the most stable. This could be explained by the fact that it is a density-based approach that relies on estimating the density

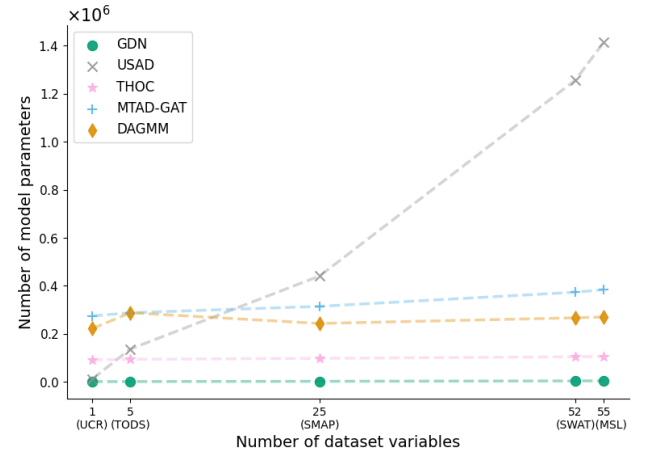


Fig. 7: Relation between the number of the parameters of the model and the number of features in the considered dataset.

of normal data. In contrast, THOC and iForest achieve less stable results, especially on SWAT.

5.4 Model size and memory consumption

Table 5 depicts the number of parameters and the model size in Mega Bytes (MB) of the tested DL architectures. GDN seems to have the lowest number of parameters when tested on all the datasets. In fact, the number of parameters in USAD is around 300 times higher than GDN. This is explained by the fact that the architecture of USAD is complex and is composed of two adversarially trained auto-encoders. In Fig. 7, it can also be seen that contrary to other models, which vary almost linearly, the number of parameters increases at a considerably higher rate. Additionally, despite the significant difference in parameter number, GDN still achieves better results than USAD. This highlights the relevance of using graph representations not only for modeling time-series but also for building less complex model architectures.

5.5 Generalization to different types of anomalies

Fig. 8 shows the percentage of detected anomalies per type for all the tested methods. In general, it can be noted that for the majority of tested techniques, collective trend anomalies are probably the most challenging to detect. ARIMA and

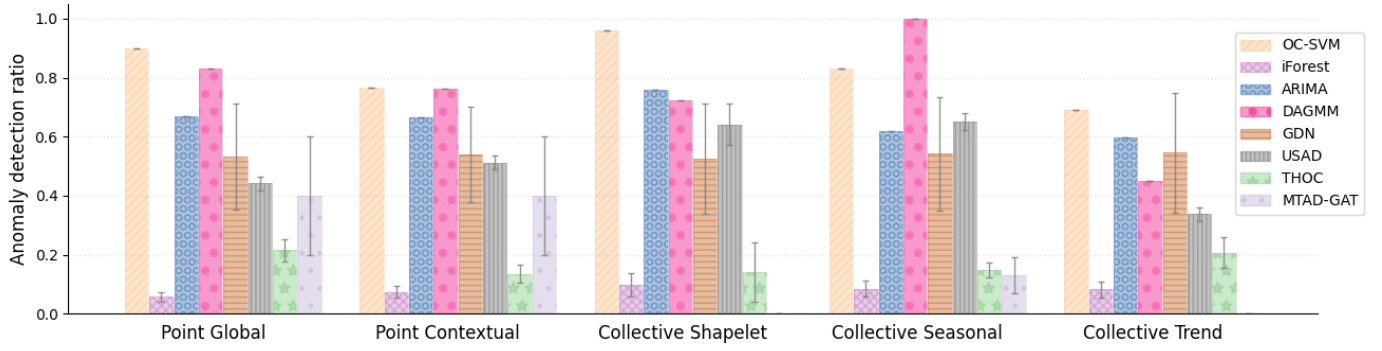


Fig. 8: The ratio of true anomalies detected for each tested method when varying the anomaly types. All methods succeeded in partially detecting each anomaly type, except MTAD-GAT which was unable to detect any collective trend anomaly.

Model	SWAT		MSL		SMAP		UCR		TODS	
	Parameters	Model size (Mb)	Parameters	Model size (Mb)	Parameters	Model size (Mb)	Parameters	Model size (Mb)	Parameters	Model size (Mb)
USAD [24]	1.256.871	4,79	1.414.755	5,40	441.225	1,68	12.321	0,05	136.710	0,54
GDN [5]	4.225	0,02	4.481	0,02	2.561	0,01	1.025	0,01	1.601	0,01
THOC [25]	104.768	0,41	105.792	0,42	98.112	0,39	91.968	0,36	94.272	0,37
MTAD-GAT [14]	373.637	1,62	384.145	1,66	314.695	1,39	274.687	1,05	288.070	1,05
DAGMM [35]	266.930	1,50	270.542	1,50	243.452	1,40	221.780	1,30	288.070	1,40

TABLE 5: Number of parameters and model size in Mega Bytes (MB) of the trained models on the different datasets

GDN, which are predictive approaches, show the best generalization capacity to different types of anomalies. OC-SVM easily detects global point and collective shapelet anomalies but still presents decent results for other anomaly types. The results obtained for USAD suggest that it is more robust to collective outliers (e.g., collective shapelet and seasonality), which can be explained by the fact that it is a reconstruction approach that can essentially capture global inconsistencies. DAGMM effectively detects collective seasonal anomalies but shows less impressive results for collective shape outliers. Again, this might return to the probabilistic nature of DAGMM, which is coupled with a sliding window. Finally, MTAD-GAT fails in detecting collective anomalies, despite being hybrid.

6 CONCLUSION

This paper proposes an extensive evaluation study of recent time-series anomaly detection methods. To the best of our knowledge, we are the first to analyze these algorithms based on a more elaborate experimentation protocol. In contrast to previous evaluation studies, which only consider the standard performance metrics, we take into account revisited performance criteria specifically designed for time series in our analysis. In addition, the model stability, the model size as well as the robustness to different types of anomalies are also investigated. All these additional elements give a more complete picture of the current state-of-the-art. Moreover, the proposed protocol is timely and could be beneficial for future investigations, providing more insights regarding their applicability in a real-world context.

ACKNOWLEDGMENT

This work is supported by the Luxembourg National Research Fund (FNR) under the projects BRIDGES2021/IS/16353350/FaKeDeTeR, UNFAKE, ref.16763798 in collaboration with POST Luxembourg and by the European Space Agency (ESA) under the project SKYTRUST 4000133885/21/NL/MH/hm.

REFERENCES

- [1] Kim, S., Choi, K., Choi, H. S., Lee, B., and Yoon, S. (2022, February). Towards a Rigorous Evaluation of Time-series Anomaly Detection. In Proceedings of the 2022 AAAI Conference on Artificial Intelligence.
- [2] Xu, H., Chen, W., Zhao, N., Li, Z., Bu, J., Li, Z., Liu, Y., Zhao, Y. Pei, Dan Feng, Y., Chen, J., Wang, Z. and Qiao, H. (2018, April). Unsupervised anomaly detection via variational auto-encoder for seasonal kpis in web applications. In Proceedings of the 2018 world wide web conference (pp. 187-196).
- [3] Choi, K., Yi, J., Park, C. and Yoon, S. (2021). Deep Learning for Anomaly Detection in Time-Series Data: Review, Analysis, and Guidelines. IEEE Access.
- [4] Schölkopf, B., Williamson, R. C., Smola, A., Shawe-Taylor, J. and Platt, J. (1999). Support vector method for novelty detection. Advances in neural information processing systems, 12.
- [5] Deng, A., and Hooi, B. (2021, February). Graph neural network-based anomaly detection in multivariate time series. In Proceedings of the AAAI Conference on Artificial Intelligence (Vol. 35, No. 5, pp. 4027-4035).
- [6] Zhao, B., Lu, H., Chen, S., Liu, J. and Wu, D. (2017). Convolutional neural networks for time series classification. Journal of Systems Engineering and Electronics, 28(1), 162-169.
- [7] Devaki, R., Kathiresan, V., Gunasekaran, S. (2014). Credit card fraud detection using time series analysis. International Journal of Computer Applications, 3, 8-10.
- [8] Jiang, J. R. and Kao, J. B. (2021). Semi-supervised time series anomaly detection based on statistics and deep learning. Applied Sciences, 11(15), 6698.
- [9] Mahalakshmi, G., Sridevi, S. and Rajaram, S. (2016, January). A survey on forecasting of time series data. In 2016 International Conference on Computing Technologies and Intelligent Data Engineering (ICCTIDE'16) (pp. 1-8). IEEE.
- [10] Golmohammadi, K. and Zaiane, O. R. (2017, August). Sentiment analysis on Twitter to improve time series contextual anomaly detection for detecting stock market manipulation. In International Conference on Big Data Analytics and Knowledge Discovery (pp. 327-342). Springer, Cham.
- [11] Tinawi, I. (2019). Machine learning for time series anomaly detection (Doctoral dissertation, Massachusetts Institute of Technology).
- [12] Hundman, K., Constantinou, V., Laporte, C., Colwell, I., and Soderstrom, T. (2018, July). Detecting spacecraft anomalies using lstms and nonparametric dynamic thresholding. In Proceedings of the 24th ACM SIGKDD international conference on knowledge discovery & data mining (pp. 387-395).
- [13] O'Neill, P., Entekhabi, D., Njoku, E., & Kellogg, K. (2010, July). The NASA soil moisture active passive (SMAP) mission: Overview.

		USAD [24]	GDN [5]	THOC [25]	MTAD-GAT [14]	DAGMM [35]	OC-SVM [4]	iForest [49]	ARIMA [36]	Avg. F1-score per dataset
SWaT	Precision _T	0.0583 ± 0.0210	0.0703 ± 0.0173	0.2905 ± 0.1113	0.0331 ± 0.0082	0.1032 ± 0.0022	0.0312 ± 0.0000	0.0038 ± 0.0014	0.0395 ± 0.0000	0.0726 ± 0.0376
	Recall _T	0.3284 ± 0.0396	0.2505 ± 0.0290	0.0204 ± 0.0108	0.3946 ± 0.0385	0.1889 ± 0.0022	0.8566 ± 0.0000	0.9021 ± 0.0014	0.8085 ± 0.0000	
	F1-Score	0.0976 ± 0.0296	0.1081 ± 0.0188	0.0381 ± 0.0196	0.0607 ± 0.0133	0.1334 ± 0.0026	0.0602 ± 0.0000	0.0077 ± 0.0029	0.0753 ± 0.0000	
MSL	Precision _T	0.1210 ± 0.0079	0.2494 ± 0.0174	0.1592 ± 0.0143	0.0768 ± 0.0045	0.1109 ± 0.0025	0.0528 ± 0.0000	0.0389 ± 0.0123	0.0843 ± 0.0000	0.0734 ± 0.0390
	Recall _T	0.2014 ± 0.0263	0.2293 ± 0.0217	0.2234 ± 0.0213	0.1846 ± 0.0045	0.0379 ± 0.0025	0.8316 ± 0.0000	0.5846 ± 0.0123	0.4106 ± 0.0000	
	F1-Score	0.0666 ± 0.0030	0.1535 ± 0.0133	0.0770 ± 0.0044	0.0319 ± 0.0023	0.0161 ± 0.0004	0.0856 ± 0.0000	0.0625 ± 0.0138	0.0937 ± 0.0000	
SMAP	Precision _T	0.1204 ± 0.0095	0.1500 ± 0.0032	0.0814 ± 0.0047	0.1401 ± 0.0000	0.0709 ± 0.0094	0.0656 ± 0.0000	0.0178 ± 0.0064	0.1401 ± 0.0000	0.0683 ± 0.0407
	Recall _T	0.2501 ± 0.0070	0.2023 ± 0.0160	0.0807 ± 0.0081	0.5272 ± 0.0000	0.0379 ± 0.0094	0.8365 ± 0.0000	0.3728 ± 0.0064	0.5272 ± 0.0000	
	F1-Score	0.0634 ± 0.0032	0.0793 ± 0.0033	0.0259 ± 0.0018	0.1179 ± 0.0000	0.0091 ± 0.0009	0.1040 ± 0.0000	0.0285 ± 0.0064	0.1179 ± 0.0000	
UCR	Precision _T	0.0106 ± 0.0002	0.0749 ± 0.0032	0.0106 ± 0.0040	0.0113 ± 0.0017	0.0709 ± 0.0094	0.0083 ± 0.0000	0.0255 ± 0.0034	0.0074 ± 0.0000	0.0176 ± 0.0147
	Recall _T	0.2320 ± 0.0023	0.2501 ± 0.0118	0.0011 ± 0.0040	0.0189 ± 0.0017	0.0379 ± 0.0094	0.8356 ± 0.0000	0.4089 ± 0.0034	0.2907 ± 0.0000	
	F1-Score	0.0168 ± 0.0003	0.0473 ± 0.0013	0.0016 ± 0.0005	0.0054 ± 0.0005	0.0091 ± 0.0009	0.0134 ± 0.0000	0.0352 ± 0.0031	0.0119 ± 0.0000	
TODS	Precision _T	0.0420 ± 0.0039	0.0537 ± 0.0130	0.0617 ± 0.0047	0.0806 ± 0.0970	0.0709 ± 0.0094	0.0197 ± 0.0000	0.0975 ± 0.0862	0.0685 ± 0.0000	0.0583 ± 0.0392
	Recall _T	0.4796 ± 0.0015	0.5546 ± 0.1713	0.1766 ± 0.0047	0.0019 ± 0.0970	0.0379 ± 0.0094	0.8054 ± 0.0000	0.0645 ± 0.0862	0.6395 ± 0.0000	
	F1-Score	0.0767 ± 0.0065	0.0843 ± 0.0147	0.0887 ± 0.0073	0.0027 ± 0.0035	0.0091 ± 0.0009	0.0382 ± 0.0000	0.0435 ± 0.0041	0.1233 ± 0.0000	
Avg. F1-score per method		0.0642 ± 0.0266	0.0945 ± 0.0353	0.0463 ± 0.0323	0.0437 ± 0.0426	0.0354 ± 0.0491	0.0603 ± 0.0324	0.0355 ± 0.0180	0.0844 ± 0.0402	

TABLE 6: The *flat-bias* performance of the tested methods on the 5 benchmarks using the metrics proposed by [59]. The average and the standard deviation of five runs are reported.

		USAD [24]	GDN [5]	THOC [5]	MTAD-GAT [14]	DAGMM [35]	OC-SVM [4]	iForest [49]	ARIMA [36]	Avg. F1-score per dataset
SWaT	Precision _T	0.0590 ± 0.0213	0.0705 ± 0.0173	0.2905 ± 0.1114	0.0312 ± 0.0076	0.1046 ± 0.0023	0.0331 ± 0.0000	0.0039 ± 0.0014	0.0404 ± 0.0000	0.0734 ± 0.0372
	Recall _T	0.3201 ± 0.0348	0.2504 ± 0.0296	0.0221 ± 0.0113	0.4632 ± 0.0480	0.1816 ± 0.0023	0.8571 ± 0.0000	0.9028 ± 0.0014	0.8119 ± 0.0000	
	F1-Score	0.0981 ± 0.0296	0.1084 ± 0.0189	0.0409 ± 0.0204	0.0580 ± 0.0129	0.1327 ± 0.0026	0.0638 ± 0.0000	0.0079 ± 0.0029	0.0771 ± 0.0000	
MSL	Precision _T	0.1210 ± 0.0081	0.2494 ± 0.0176	0.1631 ± 0.0150	0.0758 ± 0.0046	0.1110 ± 0.0025	0.0527 ± 0.0000	0.0407 ± 0.0132	0.0690 ± 0.0000	0.0705 ± 0.0384
	Recall _T	0.2114 ± 0.0262	0.2293 ± 0.0217	0.1996 ± 0.0192	0.1871 ± 0.0046	0.0291 ± 0.0025	0.8125 ± 0.0000	0.5542 ± 0.0132	0.4230 ± 0.0000	
	F1-Score	0.0671 ± 0.0023	0.1535 ± 0.0133	0.0806 ± 0.0047	0.0308 ± 0.0029	0.0156 ± 0.0005	0.0813 ± 0.0000	0.0627 ± 0.0140	0.0727 ± 0.0000	
SMAP	Precision _T	0.1202 ± 0.0095	0.1509 ± 0.0031	0.0817 ± 0.0048	0.1102 ± 0.0000	0.0708 ± 0.0094	0.0363 ± 0.0000	0.0192 ± 0.0071	0.1102 ± 0.0000	0.0544 ± 0.0277
	Recall _T	0.2634 ± 0.0079	0.1913 ± 0.0164	0.0690 ± 0.0123	0.5410 ± 0.0000	0.0388 ± 0.0094	0.8238 ± 0.0000	0.3529 ± 0.0071	0.5410 ± 0.0000	
	F1-Score	0.0642 ± 0.0025	0.0761 ± 0.0030	0.0227 ± 0.0013	0.0843 ± 0.0000	0.0090 ± 0.0011	0.0648 ± 0.0000	0.0296 ± 0.0061	0.0843 ± 0.0000	
UCR	Precision _T	0.0106 ± 0.0002	0.0753 ± 0.0030	0.0106 ± 0.0040	0.0113 ± 0.0017	0.0708 ± 0.0094	0.0079 ± 0.0000	0.0270 ± 0.0035	0.0076 ± 0.0000	0.0181 ± 0.0154
	Recall _T	0.2295 ± 0.0029	0.2510 ± 0.0109	0.0011 ± 0.0040	0.0190 ± 0.0017	0.0388 ± 0.0094	0.8286 ± 0.0000	0.3895 ± 0.0035	0.2911 ± 0.0000	
	F1-Score	0.0167 ± 0.0002	0.0496 ± 0.0010	0.0015 ± 0.0005	0.0051 ± 0.0003	0.0090 ± 0.0011	0.0145 ± 0.0000	0.0362 ± 0.0032	0.0121 ± 0.0000	
TODS	Precision _T	0.0418 ± 0.0042	0.0532 ± 0.0122	0.0620 ± 0.0042	0.0801 ± 0.097	0.0708 ± 0.0094	0.0247 ± 0.0000	0.0979 ± 0.0865	0.0679 ± 0.0000	0.0592 ± 0.0385
	Recall _T	0.4795 ± 0.0115	0.5549 ± 0.1724	0.1775 ± 0.0042	0.0019 ± 0.0970	0.0388 ± 0.0094	0.8028 ± 0.0000	0.0656 ± 0.0865	0.6396 ± 0.0000	
	F1-Score	0.0767 ± 0.0065	0.0837 ± 0.0136	0.0886 ± 0.0075	0.0023 ± 0.0035	0.0090 ± 0.0011	0.0472 ± 0.0000	0.0437 ± 0.0035	0.1222 ± 0.0000	
Avg. F1-score per method		0.0646 ± 0.0267	0.0943 ± 0.0351	0.0469 ± 0.0333	0.0361 ± 0.0314	0.0351 ± 0.0489	0.0543 ± 0.0226	0.0360 ± 0.0179	0.0737 ± 0.0354	

TABLE 7: The *front-bias* performance of the tested methods on the 5 benchmarks using the metrics proposed by [59]. The average and the standard deviation of five runs are reported.

		USAD [24]	GDN [5]	THOC [25]	MTAD-GAT [14]	DAGMM [35]	OC-SVM [4]	iForest [49]	ARIMA [36]	Avg. F1-score per dataset
SWaT	Precision _T	0.0592 ± 0.0214	0.0705 ± 0.0173	0.2905 ± 0.1113	0.0344 ± 0.0085	0.1040 ± 0.0022	0.0337 ± 0.0000	0.0040 ± 0.0015	0.0382 ± 0.0000	0.0743 ± 0.0379
	Recall _T	0.3382 ± 0.0432	0.2523 ± 0.0301	0.0217 ± 0.0131	0.4391 ± 0.0431	0.2018 ± 0.0022	0.8571 ± 0.0000	0.9028 ± 0.0015	0.8057 ± 0.0000	
	F1-Score	0.0993 ± 0.0303	0.1084 ± 0.0188	0.0401 ± 0.0236	0.0634 ± 0.0140	0.1372 ± 0.0025	0.0648 ± 0.0000	0.0080 ± 0.0030	0.0731 ± 0.0000	
MSL	Precision _T	0.1208 ± 0.0081	0.2518 ± 0.0180	0.1590 ± 0.0141	0.0760 ± 0.0046	0.1109 ± 0.0025	0.0567 ± 0.0000	0.0410 ± 0.0133	0.0831 ± 0.0000	0.0748 ± 0.0424
	Recall _T	0.2221 ± 0.0330	0.2547 ± 0.0222	0.2379 ± 0.0248	0.1846 ± 0.0046	0.0405 ± 0.0025	0.8491 ± 0.0000	0.6078 ± 0.0133	0.4078 ± 0.0000	
	F1-Score	0.0666 ± 0.0037	0.1652 ± 0.0176	0.0741 ± 0.0043	0.0301 ± 0.0023	0.0152 ± 0.0004	0.0927 ± 0.0000	0.0655 ± 0.0149	0.0891 ± 0.0000	
SMAP	Precision _T	0.1204 ± 0.0096	0.1506 ± 0.0032	0.0800 ± 0.0050	0.1363 ± 0.0000	0.0708 ± 0.0094	0.0582 ± 0.0000	0.0189 ± 0.0070	0.1363 ± 0.0000	0.0673 ± 0.0392
	Recall _T	0.2608 ± 0.0096	0.2254 ± 0.0179	0.0813 ± 0.0047	0.5403 ± 0.0000	0.0416 ± 0.0094	0.8484 ± 0.0000	0.3890 ± 0.0070	0.5403 ± 0.0000	
	F1-Score	0.0656 ± 0.0039	0.0847 ± 0.0025	0.0238 ± 0.0018	0.1146 ± 0.0000	0.0089 ± 0.0010	0.0962 ± 0.0000	0.0301 ± 0.0069	0.1146 ± 0.0000	
UCR	Precision _T	0.0104 ± 0.0002	0.0759 ± 0.0029	0.0106 ± 0.0040	0.0114 ± 0.0017	0.0708 ± 0.0094	0.0090 ± 0.0000	0.0269 ± 0.0035	0.0075 ± 0.0000	0.0176 ± 0.0141
	Recall _T	0.2375 ± 0.0024	0.2524 ± 0.0123	0.0015 ± 0.0040	0.0201 ± 0.0017	0.0416 ± 0.0094	0.8421 ± 0.0000	0.4258 ± 0.0035	0.2920 ± 0.0000	
	F1-Score	0.0165 ± 0.0003	0.0439 ± 0.0019	0.0019 ± 0.0008	0.0054 ± 0.0006	0.0089 ± 0.0010	0.0151 ± 0.0000	0.0371 ± 0.0032	0.0121 ± 0.0000	
TODS	Precision _T	0.0426 ± 0.0040	0.0541 ± 0.0131	0.0622 ± 0.0046	0.0802 ± 0.097	0.0708 ± 0.0094	0.0204 ± 0.0000	0.0972 ± 0.0862	0.0682 ± 0.0000	0.0586 ± 0.0393
	Recall _T	0.4791 ± 0.0116	0.5557 ± 0.1702	0.1772 ± 0.0046	0.0018 ± 0.0970	0.0416 ± 0.0094	0.8065 ± 0.0000	0.0645 ± 0.0862	0.6405 ± 0.0000	
	F1-Score	0.0777 ± 0.0066	0.0847 ± 0.0144	0.0894 ± 0.0073	0.0023 ± 0.0035	0.0089 ± 0.0010	0.0397 ± 0.0000	0.0434 ± 0.0039	0.1227 ± 0.0000	
Avg. F1-score per method		0.0651 ± 0.0272	0.0976 ± 0.0397	0.0459 ± 0.0321	0.0432 ± 0.0419	0.0358 ± 0.0507	0.0617 ± 0.0310	0.0368 ± 0.0187	0.0823 ± 0.0393	

TABLE 8: The *middle-bias* performance of the tested methods on the 5 benchmarks using the metrics proposed by [59]. The average and the standard deviation of five runs are reported.

		USAD [24]	GDN [5]	THOC [25]	MTAD-GAT [14]	DAGMM [35]	OC-SVM [4]	iForest [49]	ARIMA [36]	Avg. F1-score per dataset
SWaT	Precision _T	0.0576 ± 0.0208	0.0701 ± 0.0174	0.2905 ± 0.1113	0.0351 ± 0.0087	0.1018 ± 0.0022	0.0292 ± 0.000	0.0037 ± 0.0014	0.0385 ± 0.0000	0.0718 ± 0.0381
	Recall _T	0.3367 ± 0.0449	0.2505 ± 0.0286	0.0188 ± 0.0103	0.3261 ± 0.0291	0.1961 ± 0.0022	0.8561 ± 0.0000	0.9014 ± 0.0014	0.8050 ± 0.0000	
	F1-Score	0.0969 ± 0.0296	0.1078 ± 0.0187	0.0352 ± 0.0189	0.0628 ± 0.0135	0.1340 ± 0.0026	0.0565 ± 0.0000	0.0075 ± 0.0029	0.0734 ± 0.0000	
MSL	Precision _T	0.1231 ± 0.0073	0.2494 ± 0.0172	0.1553 ± 0.0137	0.0778 ± 0.0044	0.1107 ± 0.0025	0.0528 ± 0.0000	0.0372 ± 0.0114	0.0996 ± 0.0000	0.0747 ± 0.0408
	Recall _T	0.1914 ± 0.0264	0.2405 ± 0.0201	0.2471 ± 0.0245	0.1820 ± 0.0044	0.0467 ± 0.0025	0.8507 ± 0.0000	0.6151 ± 0.0114	0.3982 ± 0.0000	
	F1-Score	0.0648 ± 0.0037	0.1558 ± 0.0130	0.0706 ± 0.0037	0.0325 ± 0.0016	0.0164 ± 0.0164	0.0887 ± 0.0000	0.0613 ± 0.0137	0.1076 ± 0.0000	
SMAP	Precision _T	0.1206 ± 0.0025	0.1491 ± 0.0033	0.0811 ± 0.0047	0.1699 ± 0.0000	0.0711 ± 0.0094	0.0949 ± 0.0000	0.0164 ± 0.0057	0.1699 ± 0.0000	0.0767 ± 0.0503
	Recall _T	0.2367 ± 0.0070	0.2133 ± 0.0157	0.0923 ± 0.0042	0.5133 ± 0.0000	0.0369 ± 0.0094	0.8491 ± 0.0000	0.3927 ± 0.0057	0.5133 ± 0.0000	
	F1-Score	0.0612 ± 0.0025	0.0807 ± 0.0033	0.0275 ± 0.0022	0.1375 ± 0.0000	0.0092 ± 0.0008	0.1330 ± 0.0000	0.0270 ± 0.0065	0.1375 ± 0.0000	
UCR	Precision _T	0.0106 ± 0.0002	0.0744 ± 0.0035	0.0106 ± 0.0040	0.0114 ± 0.0017	0.0711 ± 0.0094	0.0087 ± 0.0000	0.0239 ± 0.0032	0.0073 ± 0.0000	0.0164 ± 0.0129
	Recall _T	0.2345 ± 0.0020	0.2492 ± 0.0126	0.0011 ± 0.0040	0.0188 ± 0.0017	0.0369 ± 0.0094	0.8426 ± 0.0000	0.4283 ± 0.0032	0.2903 ± 0.0000	
	F1-Score	0.0167 ± 0.0003	0.0411 ± 0.0018	0.0017 ± 0.0006	0.0054 ± 0.0006	0.0092 ± 0.0008	0.0121 ± 0.0000	0.0337 ± 0.0031	0.0116 ± 0.0000	
TODS	Precision _T	0.0421 ± 0.0039	0.0542 ± 0.0140	0.0614 ± 0.0063	0.0812 ± 0.0970	0.0711 ± 0.0094	0.0147 ± 0.0000	0.0970 ± 0.0859	0.0692 ± 0.0000	0.0573 ± 0.0401
	Recall _T	0.4796 ± 0.0116	0.5543 ± 0.1702	0.1757 ± 0.0063	0.0018 ± 0.0970	0.0369 ± 0.0094	0.8080 ± 0.0000	0.0634 ± 0.0859	0.6393 ± 0.0000	
	F1-Score	0.0769 ± 0.0065	0.0848 ± 0.0158	0.0882 ± 0.0084	0.0029 ± 0.0037	0.0092 ± 0.0008	0.0289 ± 0.0000	0.0432 ± 0.0046	0.1243 ± 0.0000	
Avg. F1-score per method		0.0633 ± 0.0264	0.0940 ± 0.0376	0.0446 ± 0.0310	0.0482 ± 0.0496	0.0356 ± 0.4993	0.0638 ± 0.0433	0.0345 ± 0.0178	0.0909 ± 0.0451	

- In 2010 IEEE International Geoscience and Remote Sensing Symposium (pp. 3236-3239). IEEE.
- [14] Zhao, H., Wang, Y., Duan, J., Huang, C., Cao, D., Tong, Y., Xu, B., Bai, J., Tong, J., and Zhang, Q. (2020, November). Multivariate time-series anomaly detection via graph attention network. In 2020 IEEE International Conference on Data Mining (ICDM) (pp. 841-850). IEEE.
 - [15] Blázquez-García, A., Conde, A., Mori, U. and Lozano, J. A. (2021). A review on outlier/anomaly detection in time series data. *ACM Computing Surveys (CSUR)*, 54(3), 1-33.
 - [16] Chen, X., Wang, H., Wei, Y., Li, J., and Gao, H. (2019). Autoregressive-Model-Based Methods for Online Time Series Prediction with Missing Values: an Experimental Evaluation. *arXiv preprint arXiv:1908.06729*.
 - [17] Jin, B., Chen, Y., Li, D., Poolla, K., & Sangiovanni-Vincentelli, A. (2019, June). A one-class support vector machine calibration method for time series change point detection. In 2019 IEEE International conference on prognostics and health management (ICPHM) (pp. 1-5). IEEE.
 - [18] Liu, F. T., Ting, K. M., and Zhou, Z. H. (2008, December). Isolation forest. In 2008 eighth IEEE international conference on data mining (pp. 413-422). IEEE.
 - [19] Yaacob, A. H., Tan, I. K., Chien, S. F., and Tan, H. K. (2010, February). Arima based network anomaly detection. In 2010 Second International Conference on Communication Software and Networks (pp. 205-209). IEEE.
 - [20] Su, Y., Zhao, Y., Niu, C., Liu, R., Sun, W. and Pei, D. (2019, July). Robust anomaly detection for multivariate time series through stochastic recurrent neural network. In Proceedings of the 25th ACM SIGKDD international conference on knowledge discovery and data mining (pp. 2828-2837).
 - [21] Wu, R. and Keogh, E. (2021). Current time series anomaly detection benchmarks are flawed and are creating the illusion of progress. *IEEE Transactions on Knowledge and Data Engineering*.
 - [22] Keogh, E., Lin, J., Fu, A. W., Van Herle, H. (2006). Finding unusual medical time-series subsequences: Algorithms and applications. *IEEE Transactions on Information Technology in Biomedicine*, 10(3), 429-439.
 - [23] Cook, A. A., Misirlı, G., Fan, Z. (2019). Anomaly detection for IoT time-series data: A survey. *IEEE Internet of Things Journal*, 7(7), 6481-6494.
 - [24] Cook, A. A., Misirlı, G., and Fan, Z. (2019). Anomaly detection for IoT time-series data: A survey. *IEEE Internet of Things Journal*, 7(7), 6481-6494.
 - [25] Shen, L., Li, Z., and Kwok, J. (2020). Timeseries anomaly detection using temporal hierarchical one-class network. *Advances in Neural Information Processing Systems*, 33, 13016-13026.
 - [26] Su, Y., Zhao, Y., Niu, C., Liu, R., Sun, W. and Pei, D. (2019, July). Robust anomaly detection for multivariate time series through stochastic recurrent neural network. In Proceedings of the 25th ACM SIGKDD international conference on knowledge discovery and data mining (pp. 2828-2837).
 - [27] Geiger, A., Liu, D., Alnegheimish, S., Cuesta-Infante, A., and Veeramachaneni, K. (2020, December). TadGAN: Time series anomaly detection using generative adversarial networks. In 2020 IEEE International Conference on Big Data (Big Data) (pp. 33-43). IEEE.
 - [28] Baptista, R., Ghorbel, E., Moissenet, F., Aouada, D., Douchet, A., André, M., ... & Bouilland, S. (2019). Home self-training: Visual feedback for assisting physical activity for stroke survivors. *Computer methods and programs in biomedicine*, 176, 111-120.
 - [29] Yu, Y., Zhu, Y., Li, S., & Wan, D. (2014). Time series outlier detection based on sliding window prediction. *Mathematical problems in Engineering*, 2014.
 - [30] Golmohammadi, K., & Zaiane, O. R. (2015, October). Time series contextual anomaly detection for detecting market manipulation in stock market. In 2015 IEEE international conference on data science and advanced analytics (DSAA) (pp. 1-10). IEEE.
 - [31] Lin, S., Clark, R., Birke, R., Schönborn, S., Trigoni, N., & Roberts, S. (2020, May). Anomaly detection for time series using vae-lstm hybrid model. In ICASSP 2020-2020 IEEE International Conference on Acoustics, Speech and Signal Processing (ICASSP) (pp. 4322-4326). IEEE.
 - [32] Reddy, K. K., Sarkar, S., Venugopalan, V., & Giering, M. (2016). Anomaly detection and fault disambiguation in large flight data: A multi-modal deep auto-encoder approach. In *Annual Conference of the PHM Society* (Vol. 8, No. 1).
 - [33] Li, D., Chen, D., Jin, B., Shi, L., Goh, J., and Ng, S. K. (2019, September). MAD-GAN: Multivariate anomaly detection for time series data with generative adversarial networks. In *International Conference on Artificial Neural Networks* (pp. 703-716). Springer, Cham.
 - [34] Malhotra, P., Vig, L., Shroff, G., & Agarwal, P. (2015, April). Long short term memory networks for anomaly detection in time series. In *Proceedings* (Vol. 89, pp. 89-94).
 - [35] Zong, B., Song, Q., Min, M. R., Cheng, W., Lumezanu, C., Cho, D., and Chen, H. (2018, February). Deep autoencoding gaussian mixture model for unsupervised anomaly detection. In *International conference on learning representations*.
 - [36] Moayedı, H. Z., & Masnadi-Shirazi, M. A. (2008, August). Arima model for network traffic prediction and anomaly detection. In 2008 international symposium on information technology (Vol. 4, pp. 1-6). IEEE.
 - [37] Baptista, R., Demisse, G., Aouada, D., & Ottersten, B. (2018, November). Deformation-based abnormal motion detection using 3d skeletons. In 2018 Eighth International Conference on Image Processing Theory, Tools and Applications (IPTA) (pp. 1-6). IEEE.
 - [38] Diab, D. M., AsSadhan, B., Binsalleh, H., Lambbotharan, S., Kyriakopoulos, K. G., & Ghafir, I. (2019, August). Anomaly detection using dynamic time warping. In 2019 IEEE International Conference on Computational Science and Engineering (CSE) and IEEE International Conference on Embedded and Ubiquitous Computing (EUC) (pp. 193-198). IEEE.
 - [39] Benkabou, S. E., Benabdeslem, K., & Canitia, B. (2018). Unsupervised outlier detection for time series by entropy and dynamic time warping. *Knowledge and Information Systems*, 54(2), 463-486.
 - [40] Berndt, D. J., & Clifford, J. (1994, July). Using dynamic time warping to find patterns in time series. In *KDD workshop* (Vol. 10, No. 16, pp. 359-370).
 - [41] Lai, K. H., Zha, D., Xu, J., Zhao, Y., Wang, G. and Hu, X. (2021, June). Revisiting time series outlier detection: Definitions and benchmarks. In *Thirty-fifth Conference on Neural Information Processing Systems Datasets and Benchmarks Track* (Round 1).
 - [42] Hyndman, R. J., Wang, E., & Laptev, N. (2015, November). Large-scale unusual time series detection. In 2015 IEEE international conference on data mining workshop (ICDMW) (pp. 1616-1619). IEEE.
 - [43] Jin, Y., Qiu, C., Sun, L., Peng, X., & Zhou, J. (2017, September). Anomaly detection in time series via robust PCA. In 2017 2nd IEEE International Conference on Intelligent Transportation Engineering (ICITE) (pp. 352-355). IEEE.
 - [44] Wang, X., Miranda-Moreno, L., & Sun, L. (2021). Hankel-structured Tensor Robust PCA for Multivariate Traffic Time Series Anomaly Detection. *arXiv preprint arXiv:2110.04352*.
 - [45] Oja, E. (1982). Simplified neuron model as a principal component analyzer. *Journal of mathematical biology*, 15(3), 267-273.
 - [46] Kirby, M., & Sirovich, L. (1990). Application of the Karhunen-Loeve procedure for the characterization of human faces. *IEEE Transactions on Pattern analysis and Machine intelligence*, 12(1), 103-108.
 - [47] Schölkopf, B., Smola, A., & Müller, K. R. (1998). Nonlinear component analysis as a kernel eigenvalue problem. *Neural computation*, 10(5), 1299-1319.
 - [48] Ruff, L., Vandermeulen, R., Goernitz, N., Deecke, L., Siddiqui, S.A., Binder, A., Müller, E., and Kloft, M., Deep one-class classification. In *International Conference on Machine Learning*, pages 4393-4402, 2018.
 - [49] Liu, F. T., Ting, K. M., and Zhou, Z. H. (2008, December). Isolation forest. In 2008 eighth IEEE international conference on data mining (pp. 413-422). IEEE.
 - [50] Breunig, M. M., Kriegel, H. P., Ng, R. T., & Sander, J. (2000, May). LOF: identifying density-based local outliers. In *Proceedings of the 2000 ACM SIGMOD international conference on Management of data* (pp. 93-104).
 - [51] Yairi, T., Takeishi, N., Oda, T., Nakajima, Y., Nishimura, N., & Takata, N. (2017). A data-driven health monitoring method for satellite housekeeping data based on probabilistic clustering and dimensionality reduction. *IEEE Transactions on Aerospace and Electronic Systems*, 53(3), 1384-1401.
 - [52] Lindstrom, M. R., Jung, H., & Larocque, D. (2020). Functional Kernel Density Estimation: Point and Fourier Approaches to Time Series Anomaly Detection. *Entropy*, 22(12), 1363.
 - [53] Tang, J., Chen, Z., Fu, A. W. C., & Cheung, D. W. (2002, May). Enhancing effectiveness of outlier detections for low density pat-

terns. In Pacific-Asia conference on knowledge discovery and data mining (pp. 535-548). Springer, Berlin, Heidelberg.

- [54] Tax, D. M., & Duin, R. P. (2004). Support vector data description. *Machine learning*, 54(1), 45-66.
- [55] Huang, C., Min, G., Wu, Y., Ying, Y., Pei, K., & Xiang, Z. (2017). Time series anomaly detection for trustworthy services in cloud computing systems. *IEEE Transactions on Big Data*.
- [56] Li, K. L., Huang, H. K., Tian, S. F., & Xu, W. (2003, November). Improving one-class SVM for anomaly detection. In *Proceedings of the 2003 international conference on machine learning and cybernetics (IEEE Cat. No. 03EX693) (Vol. 5, pp. 3077-3081)*. IEEE.
- [57] Wang, Y., Wong, J., & Miner, A. (2004, June). Anomaly intrusion detection using one class SVM. In *Proceedings from the Fifth Annual IEEE SMC Information Assurance Workshop, 2004.* (pp. 358-364). IEEE.
- [58] Ma, J., & Perkins, S. (2003, July). Time-series novelty detection using one-class support vector machines. In *Proceedings of the International Joint Conference on Neural Networks, 2003.* (Vol. 3, pp. 1741-1745). IEEE.
- [59] Tatbul, N., Lee, T. J., Zdonik, S., Alam, M., & Gottschlich, J. (2018). Precision and recall for time series. *Advances in neural information processing systems*, 31.
- [60] Musallam, M. A., Gaudilliere, V., Ghorbel, E., Al Ismaeil, K., Perez, M. D., Poucet, M., & Aouada, D. (2021, September). Spacecraft Recognition Leveraging Knowledge of Space Environment: Simulator, Dataset, Competition Design and Analysis. In *2021 IEEE International Conference on Image Processing Challenges (ICIPC)* (pp. 11-15). IEEE.
- [61] Granger, C. W., & Watson, M. W. (1984). Time series and spectral methods in econometrics. *Handbook of econometrics*, 2, 979-1022.
- [62] L. Zhang, R. Cushing, C. d. Laat and P. Grosso, "A real-time intrusion detection system based on OC-SVM for containerized applications," *2021 IEEE 24th International Conference on Computational Science and Engineering (CSE)*, 2021, pp. 138-145, doi: 10.1109/CSE53436.2021.00029.
- [63] M. A. Siddiqui et al., "Detecting Cyber Attacks Using Anomaly Detection with Explanations and Expert Feedback," *ICASSP 2019 - 2019 IEEE International Conference on Acoustics, Speech and Signal Processing (ICASSP)*, 2019, pp. 2872-2876, doi: 10.1109/ICASSP.2019.8683212.



Nesryne Mejri is currently a Ph.D. student at the Computer Vision, Imaging and Machine Intelligence (CVI2) Research Group at the Interdisciplinary Centre for Security, Reliability, and Trust (SnT), University of Luxembourg. She received the M.Sc degree in Information and Computer Science from the University of Luxembourg, in 2021. Her research interests are in Computer Vision and Deep Learning.



Laura Lopez Fuentes holds a M.Sc in Computer Vision from the Autonomous university of Barcelona. She received her Ph.D. in Computer Vision from the University of the Balearic Islands (Spain) in 2021. Her Ph.D. was in collaboration with the Computer Vision Center of Barcelona and the company AnsuR Technologies based in Oslo (Norway). In 2021, Dr. Lopez joined the University of Luxembourg in the Computer Vision, Imaging, and Machine Intelligence Research Group.



Kankana Roy received the B.Tech. degree in Computer Science and Engineering from the West Bengal University of Technology, Kolkata, India, in 2011, the M.Tech. in Computer Science and Engineering from the National Institute of Technology, Durgapur, India, in 2013 and Ph.D. degree from the Indian Institute of Technology Kharagpur, India, in 2021. She was employed as a software engineer at the NRI Financial Technologies from 2013 to 2015. She was a research associate at University of Luxembourg, from 2020 to 2021. Her research interests include computer vision, dictionary learning, human computer interaction, and machine learning.



Pavel Chernakov is currently an B.Sci. student in Information and Computer Science at the University of Luxembourg. He had several research internships at the Computer Vision, Imaging and Machine Intelligence (CVI2) Research Group. His interests include computer vision, cybersecurity and software development.



Enjie Ghorbel is Research Scientist at the Interdisciplinary Centre for Security, Reliability, and Trust (SnT), University of Luxembourg. She received her engineering diploma from the National Engineering School of Sousse (ENISO) in Applied Computer Science in 2014 and her PhD in Computer Science, from the University of Normandie, in 2017. Her research interests include computer vision and pattern recognition.



Djamila Aouada is Senior Research Scientist and Assistant Professor at the Interdisciplinary Centre for Security, Reliability, and Trust (SnT), University of Luxembourg. She is Head of the Computer Vision, Imaging and Machine Intelligence (CVI2) Research Group at SnT, and Head of the SnT Computer Vision Laboratory and co-Head of the SnT Zero-G Laboratory. Dr. Aouada received the State Engineering degree in electronics in 2005, from the École Nationale Polytechnique (ENP), Algiers, Algeria, and the Ph.D. degree in electrical engineering in 2009 from North Carolina State University (NCSU), Raleigh, NC, USA. Dr. Aouada has worked as a consultant for multiple renowned laboratories (Los Alamos National Laboratory, Alcatel Lucent Bell Labs., and Mitsubishi Electric Research Labs.). She has been leading the computer vision activities at SnT since 2009. Her research interests span the areas of image processing, computer vision, and data modelling. Dr. Aouada is Senior Member of the IEEE, member of the IEEE Signal Processing Society, IEEE WIE, INSTICC and the Eta Kappa Nu honor society (HKN). She has served as the Chair of the IEEE Benelux Women in Engineering Affinity Group from 2014 to 2016, Chair of the SHARP workshop at ECCV 2020, CVPR 2021 and CVPR 2022, Area Chair at 3DV 2020 and 2022 and Program Chair at 3DV 2021, General Chair at RTIP2R 2022, and Program Chair at EUVIP 2023. She is the recipient of four IEEE best paper awards.